Supplemental Material

Emergence of a Landau level structure in dark optical lattices

S1. The non-degeneracy condition of OFLs

In its simplest version [3], an optical flux lattice (OFL) consists in a spatially periodic coupling between two internal states $|a\rangle$ and $|b\rangle$ (not necessarily the two states $|g_+\rangle$ and $|g_-\rangle$ introduced in the main text). This coupling can be written $\hat{V} = \epsilon_0 \hat{1} + \epsilon_1 \, \boldsymbol{n} \cdot \hat{\boldsymbol{\sigma}}$, where the real functions $\epsilon_0(\boldsymbol{r})$, $\epsilon_1(\boldsymbol{r})$ and the unit vector $\boldsymbol{n}(\boldsymbol{r})$ are spatially periodic, and the $\hat{\sigma}_j$ $(j = x, y, z)$ are the Pauli matrices.

At any point in space, we can diagonalize $\hat{V}$ and obtain the two eigenstates $|\pm\rangle_{\boldsymbol{n}}$ with the energies $\epsilon_0 \pm \epsilon_1$. The non-degeneracy condition stated in [3] imposes that ϵ_1 does not cancel at any point in the unit cell. Suppose for example that ϵ_1 is strictly positive everywhere, and consider the Berry connection $\boldsymbol{A}(\boldsymbol{r}) = \mathrm{i}\hbar \, {}_{\boldsymbol{n}}\langle -|\boldsymbol{\nabla}\,(|-\rangle_{\boldsymbol{n}})$ and the Berry curvature $B_z(\boldsymbol{r}) = (\boldsymbol{\nabla} \times \boldsymbol{A})_z$ that emerge for an adiabatic following of the local ground state $|-\rangle_{\boldsymbol{n}}$. By definition of an OFL, the flux of B_z across the unit cell should be non-zero. Using Stokes theorem, this flux is given by:

$$\iint B_z \, \mathrm{d}^2 r = \oint_{\mathcal{C}} \boldsymbol{A} \cdot \mathrm{d}\boldsymbol{r} + \text{singular contributions}, \quad \text{(S1)}$$

where the contour $\mathcal{C}$ represents the edge of the unit cell. Since $\boldsymbol{A}$ is periodic on the lattice, its contour integral along the cell edge is zero and one is left with only the contribution of singularities [3, 4]. One must therefore engineer these singularities such that their sum gives a non-zero result.

Let us choose a gauge, for example $|-\rangle_{\boldsymbol{n}} = (-\mathrm{e}^{-\mathrm{i}\phi}\sin(\theta/2), \cos(\theta/2))^T$ where the spherical angles (θ, ϕ) define the orientation of $\boldsymbol{n}$. The Berry connection then reads $\boldsymbol{A} = \hbar \sin^2(\theta/2)\, \boldsymbol{\nabla}\phi$, showing that a singularity of $\boldsymbol{A}$ can appear where ϕ is ill-defined. This occurs at the zeroes of the complex periodic function $V_{ab} = \epsilon_1 \, \mathrm{e}^{-\mathrm{i}\phi} \cos\theta$, hence at places where $\theta = 0$ or π. More precisely, a point where $\theta = \pi$, i.e. $V_{aa} - \epsilon_0 = \epsilon_1 \cos\theta < 0$ will lead to a singular contribution since $\boldsymbol{A} = \hbar \boldsymbol{\nabla}\phi$ at this point, whereas $\boldsymbol{A}$ will vanish at a point where $\theta = 0$, i.e. $V_{aa} - \epsilon_0 > 0$, and there will be no contribution to Eq. (S1) in this case.

The theory of complex functions indicates that the zeroes of V_{ab} come by pairs, with an opposite circulation of the phase ϕ around the two zeroes of the pair. If $V_{aa} - \epsilon_0$ keeps the same sign at the location of the two zeroes, the singular contributions to Eq. (S1) of the two members of the pair thus compensate each other. To obtain a non-zero flux through the unit cell of the OFL, there must be at least one pair of zeroes of V_{ab} that is "rectified", i.e., for which $V_{aa} - \epsilon_0$ changes sign (hence θ switches from 0 to π) between the two pair members.

Consider now the coupling $\hat{V}(\boldsymbol{r})$ given in Eq. (1). The off-diagonal matrix element $V_{ab}(\boldsymbol{r}) = V_0 \, \alpha_+^*(\boldsymbol{r})\alpha_-(\boldsymbol{r})$ vanishes at the zeroes of the two coefficients $\alpha_\pm$. If the zeroes of α_+ and α_- do not overlap, then the rectification described above cannot operate. All zeroes of α_+ lead to a positive sign of $V_{aa} - \epsilon_0 = V_0(|\alpha_-|^2 - |\alpha_+|^2)/2$ and their contributions to Eq. (S1) thus compensate. Similarly all zeroes of α_- lead to a negative sign of $V_{aa} - \epsilon_0$, hence no contribution to Eq. (S1) either: one cannot reach a non-zero flux in this case. The only way to circumvent this conclusion is to allow at least some partial overlap between the zeroes of α_+ and α_-. However in this case, $\hat{V}$ vanishes at these common zeroes, and the two eigenstates of $\hat{V}$ coincide. As we show in the main text, this local degeneracy does not prevent the achievement of a series of topological bands.

S2. Ideal Chern band character

Recent theoretical developements introduced a class of 'ideal' Chern bands, which share the same algebraic structure as Landau levels despite a non-uniform Berry curvature [27, 36, 40, 41]. These bands are characterized by a specific structure of the quantum geometrical tensor $[\mathcal{Q}_{n,\boldsymbol{q}}]$, defined by

$$[\mathcal{Q}_{n,\boldsymbol{q}}]_{ij} = \langle \partial_{q_i}\psi_{n,\boldsymbol{q}}|(1 - |\psi_{n,\boldsymbol{q}}\rangle\langle\psi_{n,\boldsymbol{q}}|)|\partial_{q_j}\psi_{n,\boldsymbol{q}}\rangle,$$

where $|\psi_{n,\boldsymbol{q}}\rangle$ is the Bloch state of band n and quasi-momentum $\boldsymbol{q}$.

In the case of Landau levels, each band is characterized by a uniform quantum geometrical tensor given by the matrix form

$$[\mathcal{Q}_{n,\boldsymbol{q}}] = \frac{\ell^2}{2}\begin{pmatrix} 1 & -\mathrm{i} \\ \mathrm{i} & 1 \end{pmatrix},$$

where ℓ is the magnetic length. It satisfies the identity $[\mathcal{Q}_{n,\boldsymbol{q}}]\boldsymbol{\epsilon}_- = \boldsymbol{0}$ (where $\boldsymbol{\epsilon}_\pm = (\boldsymbol{e}_x \pm \mathrm{i}\,\boldsymbol{e}_y)/\sqrt{2}$), which physically means that the dynamics of the momentum component $q_x - \mathrm{i}q_y$ is suppressed. This property is at the heart of the possibility to write Landau levels wavefunctions in terms of holomorphic functions.

More generally, ideal Chern bands are characterized by the existence of a constant null vector $\boldsymbol{w}$, i.e. $[\mathcal{Q}_{n,\boldsymbol{q}}]\boldsymbol{w} = \boldsymbol{0}$ for all $\boldsymbol{q}$, which provides the same algebraic structure than Landau levels [36].

For the ground band $n = 0$ of our OFL, we find that the circular vector $\boldsymbol{w} = \boldsymbol{\epsilon}_-$ acts as an null vector to a very good approximation (on average over the band, we find $||[\mathcal{Q}_{0,\boldsymbol{q}}]\boldsymbol{\epsilon}_-|| = 0.04||[\mathcal{Q}_{0,\boldsymbol{q}}]\boldsymbol{\epsilon}_+||$ for $V_0 = 100\hbar\omega_c$). One then expects a strong analogy between our OFL ground band and the lowest Landau level, from the algebraic description of generic wavefunctions to the physical properties of the expected many-body ground states.

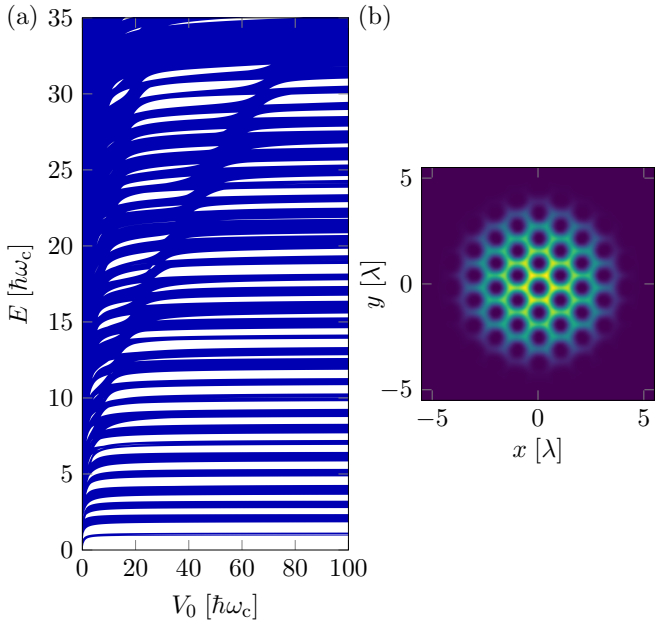

FIG. S1. (a) Bandspectrum of a dark-state OFL with a triangular symmetry, given in Eq. (S2). We recognize a series of almost equally-spaced bands at low energy, akin to Landau levels. (b) Density profile of a Bose-Einstein condensate in the OFL with triangular symmetry. We used a light shift amplitude $V_0 = 100\,\hbar\omega_c$, an interaction strength $gN/\lambda^2 = 5\,\hbar\omega_c$, and a harmonic trap frequency $\omega_{\rm trap} = 0.04\,\omega_c$.

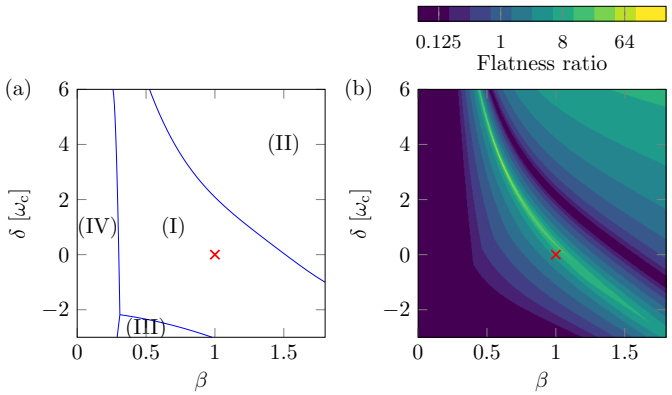

FIG. S2. (a) Phase diagram for the ground energy band of the OFL as a function of the parameters β and h_z for $V_0 = 100\,\hbar\omega_c$. The phase (I) exhibits a gapped ground band with a Chern number $\mathcal{C} = 1$. The phases (II) and (III) are both gapped with a Chern number $\mathcal{C} = 0$. In the phase (IV), the ground band overlaps with excited Bloch bands. The blue lines indicate the gapless transition lines separating the different phases. (b) Evolution of the flatness ratio with β and δ. The red cross corresponds to the values $\beta = 1$ and $\delta = 0$ considered in the main text. A maximum flatness ratio of about 130 is obtained for $\beta = 0.65$ and $\delta = 2.9\,\omega_c$ (barely visible on the plot due the strong sensitivity of high flatness ratios to β and δ).

S3. Triangular version of the dark-state lattice

We focused in the main text on a square version of the lattice. We show in this appendix that the same idea can be implemented in a triangular geometry. Consider the lattice formed by superposing three standing waves in the xy plane, superimposed with a running wave propagating along the z axis, so that the amplitudes $\alpha_\pm$ entering in the coupling matrix $\hat{V}$ of Eq. (1) read:

$$\begin{aligned} \alpha_+ &= c_1 + c_2 + c_3 + \tfrac{3}{2} \\ \alpha_- &= c_1 - \tfrac{1}{2}(c_2 + c_3) + \mathrm{i}\tfrac{\sqrt{3}}{2}(c_2 - c_3) \end{aligned} \qquad \text{(S2)}$$

where $c_i = \cos(\boldsymbol{k}_i \cdot \boldsymbol{r})$ and the wave vectors $\boldsymbol{k}_i$ are at 120° from each other. The zeros of α_- are found at two sets of points. The first one corresponds to the locations where all $c_j = 1$, the second one to the locations where all $c_j = -1/2$. The second set coincides with the locations of the zeroes of α_+, so that the coupling matrix $\hat{V}$ vanishes at these points. We recall that this local degeneracy is required for a dark-state based OFL (see appendix S1).

We show in Fig. S1a the energy spectrum as a function of the light coupling strength V_0. For large enough V_0, we find a series of almost equally-spaced energy bands, with a spacing $\hbar\omega_c = \sqrt{3}\hbar^2k^2/(2\pi m)$ consistent with the cyclotron frequency expected for the magnetic flux density. For $V_0 = 100\,\hbar\omega_c$, we find a topological lowest band with a flatness ratio $\simeq 5$. An example of Bose-Einstein condensate with a triangular vortex lattice in this configuration is shown in Fig. S1b.

S4. Topological robustness of the ground band

The lattice considered in the main text, described by Eqs. (1-3), depends only on the parameter V_0. Moreover the low-energy band structure is essentially independent of V_0 for large values of this parameter (see Fig. 1). We consider here the sensitivity of our results to different kinds of imperfections, namely a modification of the light field profile and an external magnetic field. More specifically, we consider light field amplitudes α_+ and α_- given by

$$\alpha_+(\boldsymbol{r}) = \sin X + \mathrm{i}\sin Y, \qquad \text{(S3)}$$

$$\alpha_-(\boldsymbol{r}) = \beta(\cos X + \cos Y), \qquad \text{(S4)}$$

parametrized by β. We also study the influence of a magnetic field along z giving rise to a Zeeman splitting $\hbar\delta\hat{\sigma}_z/2$. Equivalently, such a splitting also arises from a detuning δ with respect to the Raman resonance. The band structure presented in the main text correspond to the values $\beta = 1$ and $\delta = 0$.

We first consider the phase diagram of the system, more specifically the topological nature of the ground band. As shown in Fig. S2a, we find a gapped topological band with Chern number $\mathcal{C} = 1$ for a wide range of parameters around $(\beta, \delta) = (1, 0)$ (phase I). When in-

creasing the magnitude of the Zeeman field, one finds transition lines at which the gap to the first excited band vanishes, marking the transition to non-topological bands (phases II and III). For weak values of β, the system becomes metallic (phase IV).

We then consider the flatness ratio of the lowest band, i.e., the ratio of the gap to the first excited band and the width of this lowest band (see Fig. S2b). Fine tuning of the parameters β and δ allows to flatten the ground band significantly, with flatness ratios exceeding 100. This fine tuning should ease the reach of fractional quantum Hall states, for which the interaction energy dominates over the kinetic energy (i.e. the band width).